Mathematical modeling of cochlear mechanics

Stephen T. Neely
Boys Town National Institute for Communication Disorders in Children, 555 North 30th Street, Omaha, Nebraska 68131

(Received 1 January 1984; accepted for publication 22 February 1985)

The recent discovery of oto-acoustic emissions [see Zurek, J. Acoust. Soc. Am. **78**, 340–344 (1985)] and the newer measures of the micromechanics of the inner ear have generated renewed interest in quantitative descriptions of the biomechanics of the cochlea. Active elements (mechanical force generators) are thought to be essential for producing the high sensitivity and sharp tuning typically associated with normal cochlear function. A mechanical model with active elements is described which can simulate basilar membrane displacements with neural-like tuning and peak amplitudes of about 1 nm at the threshold of hearing. In addition, such models might help explain the source of oto-acoustic emissions. The paper describes the power of the recent attempts at providing quantitative descriptions and predictions of the mechanics of the cochlea.

PACS numbers: 43.10.Ln, 43.63.Bq, 43.63.Kz

INTRODUCTION

The cochlea is the principal sensory organ of the mammalian auditory system. It is one of the most intricate and least understood mechanical systems in the body. Mathematical models of the cochlea have been important tools in understanding the function of the cochlea because direct observation of cochlear vibrations is difficult. This paper outlines mathematical modeling of cochlear mechanics by describing some useful methods, recent developments, and areas needing further research.

It is convenient to consider cochlear macromechanics and micromechanics separately. Macromechanics deals with the dynamics of the fluid in the cochlear channels. Micromechanics deals with motion of the basilar membrane and tectorial membrane, including "second filters" and "active elements." The macromechanics and micromechanics are coupled in that they specify complementary constraints on the relationship between *pressure difference* across the basilar membrane and *displacement* of the basilar membrane.

The primary goal of cochlear modeling is to improve our understanding of cochlear function. Part of the art of mathematical modeling lies in choosing appropriate simplifying assumptions and approximations in order to maintain both mathematical tractibility and realistic representation of the essential cochlear features. Some results from a linear, active, time-domain cochlear model will be compared with typical measured responses of single auditory nerve fibers.

I. BACKGROUND

The inner ear consists of the cochlea, the vestibule, and three semicircular canals; these structures are communicating, fluid-filled spaces within the temporal bone. The cochlea is the primary receptor organ for hearing; it receives acoustic signals from the middle-ear ossicles and distributes sound information to individual auditory nerve fibers.

The cochlea is a tapered tube which is coiled spirally and gets its name from its resemblance to a snail. The cochlear chamber is divided into three ducts: an upper duct (scala vestibuli), a lower duct (scala tympani), and a central duct (scala media). The separation between scala media and scala vestibuli (Reissner's membrane) provides a chemical barrier, but is probably not important to cochlear mechanics. The partition between scala media and scala tympani (organ of Corti) contains the final receptor cells (inner hair cells) and plays an important role in cochlear mechanics.

The cochlear partition is mechanically tuned such that higher frequency tones cause localized vibrations nearer to the stapes. The stiffness of the partition comes primarily from the basilar membrane which spans the gap between scala media and scala tympani. The sensory hair cells are situated on the basilar membrane and move as the basilar membrane moves. Over the top of the hair cells lies the tectorial membrane. When the cochlear partition vibrates, a shearing motion between the basilar and tectorial membranes will bend the tufts of hair (stereocilia) at the top of the hair cells. The bending of the stereocilia modulates intracellular potential, thereby accomplishing mechanical-to-electrical transduction.

Mathematical models of cochlear mechanics are often used to test theories about cochlear function. One-dimensional (transmission line) models helped establish the traveling-wave character of basilar membrane motion (Zwislocki, 1950; Peterson and Bogert, 1950). Nonlinear models help to explain the generation and propagation of distortion signals in the cochlear (Kim *et al.*, 1973; Hall, 1974; Matthews, 1980). Cochlear frequency analysis and sensitivity are being investigated with cochlear models by the addition of "second filters" and active elements to the cochlear partition (Allen, 1977; Zwislocki and Kletsky, 1979; Neely and Kim, 1983). For additional background on mathematical models of cochlear mechanics, the review papers of de Boer (1980, 1984) are recommended.

II. COCHLEAR MACROMECHANICS

The effects of fluid viscosity and compressibility are generally considered to be much less important than the in-

 0001-4966/85/070345-08$00.80

ertial properties of the cochlear fluid (Viergever, 1980). The influence of the spiral curvature of the cochlear channels is also considered to be relatively unimportant (Loh, 1983). By ignoring these effects and assuming constant rectangular cochlear cross sections, cochlear macromechanics reduces the problem to solving for the pressure distribution in a rectangular box, divided into upper (scala vestibuli) and lower (scala tympani) halves by a partition (primarily the basilar membrane) and filled with an incompressible, inviscid fluid (see Fig. 1). By invoking the additional assumption that the upper and lower channels are geometrically symmetric about the partition, the problem can be formulated within a single cochlear chamber.

Let p represent the difference in pressure between the upper channel p_{uc} and lower channel p_{lc}:

$$p(x, y, z) = p_{lc}(x, y, -z) - p_{uc}(x, y, z). \tag{1}$$

In addition to the three spatial variables x, y, and z, p will also be a function of either time or frequency depending on the chosen formulation.

The pressure difference p must satisfy Laplace's equation in the fluid and appropriate constraints at the boundaries. The basic equation for cochlear macromechanics may be written as

$$\nabla^2 p \equiv \frac{\partial^2 p}{\partial x^2} + \frac{\partial^2 p}{\partial y^2} + \frac{\partial^2 p}{\partial z^2} = 0 \tag{2}$$

within the fluid, i.e., for $0 < x < L$, $0 < y < W$, $0 < z < H$. The pressure distribution must be smoothly varying with no local maxima or minima except at the channel boundaries.

At the boundaries the fluid moves with the same motion as the immediately adjacent wall. The basal wall is moving with acceleration $\ddot{\xi}_s\, \eta(y,z)$:

$$\frac{\partial}{\partial x} p(0,y,z) = 2\rho \ddot{\xi}_s \eta(y,z), \tag{3}$$

and the apical wall does not move:

$$\frac{\partial}{\partial x} p(L,y,z) = 0. \tag{4}$$

The side walls are both motionless:

$$\frac{\partial}{\partial y} p(x,0,z) = 0 \tag{5}$$

and

$$\frac{\partial}{\partial y} p(x,W,z) = 0. \tag{6}$$

The partition boundary moves with acceleration $\ddot{\xi}_1(x)\zeta(y)$:

$$\frac{\partial}{\partial z} p(x,y,0) = 2\rho \ddot{\xi}_1(x)\zeta(y), \tag{7}$$

and the upper wall does not move:

$$\frac{\partial}{\partial z} p(x,y,H) = 0. \tag{8}$$

Typically, we are interested in solving for $\xi_1(x)$ given ρ, η, ξ_s, and ζ and an additional equation from cochlear micromechanics describing the relation between $p(x,y,0)$ and $\xi_1(x)$. Alternatively, we can specify the stimulus at the eardrum, taking into account the mechanics of the middle ear and round window simultaneously with the mechanics of the cochlea (e.g., Matthews, 1983).

The dimensionless function $\zeta(y)$ represents the cross-sectional shape of the cochlear partition (bending mode) when it is displaced from its rest position at $z = 0$. If we consider ζ to be a centered half-cosine of width B (de Boer, 1981; Lighthill, 1981)

$$\zeta(y) = \begin{cases} \dfrac{\pi W}{4B} \cos\left(\dfrac{\pi y}{2B}\right), & \dfrac{-B}{2} < y < \dfrac{B}{2}, \\ 0, & \text{elsewhere.} \end{cases} \tag{9}$$

The shape of the bending mode is illustrated in Fig. 2.

The cochlear fluid influences the motion of the basilar membrane in two ways. First, the fluid provides the primary medium for propagation of acoustic energy throughout the length of the cochlea; the micromechanical constraints will generally specify little or no longitudinal coupling within the cochlear partition. Second, the fluid adds a mass to the cochlear partition dynamics. The quantity of mass that "rides" with the partition varies with the spatial wavelength in the x dimension of partition displacement; a relatively large amount of fluid mass rides with the partition when wavelengths are long, and a relatively small amount rides when wavelengths are small.

The quantity of fluid mass that rides with the partition can be derived analytically for simple cochlear geometries

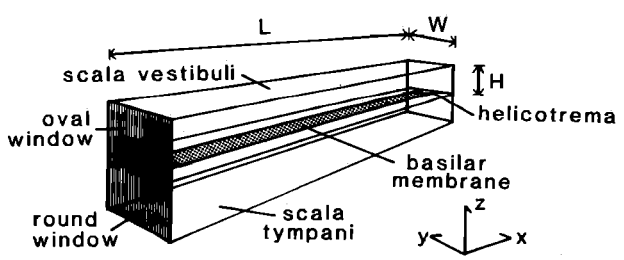

FIG. 1. Geometry of the three-dimensional model of the cochlea. The "box" has uniform, rectangular cross section and is divided into symmetric upper (scala vestibuli) and lower (scala tympani) channels by a partly flexible partition. The box has length L in the x dimension, width W in the y dimension, and height H in the z dimension.

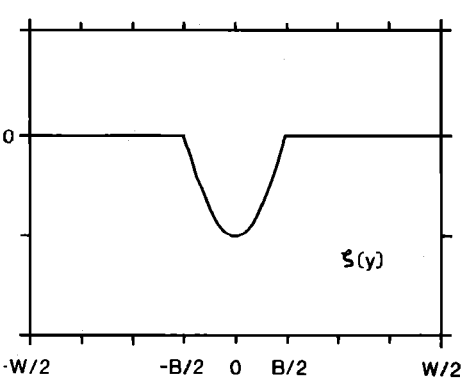

FIG. 2. Bending mode for the cochlear partition. The function $\zeta(y)$ represents the shape assumed in the model for displacement of the cochlear partition. The partition spans the entire width of the box $-W/2 \leqslant y \leqslant W/2$. The movable part of the partition is the basilar membrane, shown here with the shape of a centered, half-cosine of width B.

(Steele and Taber, 1979; de Boer, 1981; Lighthill, 1981) and gives insight into the effects of cochlear geometry and dimensionality of fluid dynamics. We will consider a nondimensional function $Q(k)$, which is proportional to the fluid inertial loading on the cochlear partition when displacement of the partition varies as $\cos(kx)$. The variable k is the wavenumber or spatial frequency in the x dimension. The function $Q(k)$ can be thought of as being proportional to the ratio of the spatial Fourier transforms of *pressure difference* and *partition acceleration*.

It can be shown (see Appendix A) that for the three-dimensional (3D), rectangular box model described above,

$$Q_{3D}(k) = \sum_{m=-\infty}^{\infty} \left(\frac{\zeta_m}{\zeta_0}\right)^2 \times \sum_{l=-\infty}^{\infty} \frac{1}{(kH)^2 + (l\pi)^2 + (m\pi H/W)^2}, \quad (10)$$

where

$$\zeta_m = \frac{1}{W}\int_{-W/2}^{W/2} \zeta(y)\cos\left(\frac{m\pi}{W}y\right)dy. \quad (11)$$

Using the example of ζ given by Eq. (9), the Fourier components ζ_m can be computed.

$$\frac{\zeta_m}{\zeta_0} = \cos\left(\frac{m\pi}{2}\right)\cos\left(\frac{m\pi B}{2W}\right)\left[1-\left(\frac{mB}{W}\right)^2\right]^{-1}. \quad (12)$$

The function $Q(k)$ incorporates the constraints imposed by the model equations on the macromechanics of the cochlear cross section.

One- and two-dimensional approximations for the cochlear box can be understood in terms of their effects on $Q(k)$. A common two-dimensional (2D) approximation (Lesser and Berkley, 1972; Allen, 1977; Neely, 1981) assumes that pressure is constant in the y dimension (i.e., $\zeta_m = 0$ for $m \neq 0$). The corresponding $Q(k)$ for this 2-D model is

$$Q_{2D}(k) = \sum_{l=-\infty}^{\infty} \frac{1}{(kH)^2 + (l\pi)^2}. \quad (13)$$

A one-dimensional (1D) long-wave approximation can be obtained from Q_{2D} by assuming small wavenumbers (wavelength much larger than the cross section of the channel) in addition to the previous assumption of constant pressure in the y dimension [i.e., $(kh)^2 \ll (l\pi)^2$ and $\zeta_m = 0$ for $m \neq 0$]. The corresponding $Q(k)$ for this 1-D model is

$$Q_{1D} = 1/(kH)^2 + 1/3. \quad (14)$$

The constant $1/3$ is a result of summing the series in Eq. (13) over $l \neq 0$ and with $(kH)^2 = 0$. This constant can be interpreted as a fixed amount of mass riding with the partition. The 1-D and 2-D approximations for $Q(k)$ are also illustrated in Fig. 3.

The above series representations for $Q(k)$ can be transformed into ordinary differential equations in the x dimension. For example, Eq. (14) defines an ordinary differential equation of second order in x for the 1-D long-wave approximation (see Appendix B). Another approximation method, suggested by de Boer and van Bienema (1983), is based on curve fitting the Q_{3D} function. For example, a better curve fit (by sight) to $Q_{3D}(k)$ would be

$$Q_6(k) = \frac{1}{(kH)^2} + \frac{2.4}{(kH)^2 + \pi^2} + \frac{12}{(kH)^2 + (4\pi)^2} + 0.12, \quad (15)$$

which defines an ordinary differential equation of order six in x. This approximation is also shown graphically in Fig. 3.

In addition to the differential equation methods, integral equation methods may also be derived from $Q(k)$. For a time-domain formulation, if partition mass is assumed to be constant for all x, then a spatial Green function can be obtained from $Q(k)$ which, when convolved with a function of known variables at each time step, will provide the partition acceleration needed to extrapolate velocity and displacement to the next time step. The convolution may be computed directly in the x dimension (Matthews, 1980) or in the spatial frequency (wavenumber) domain through use of the fast Fourier transform (Allen and Sondhi, 1979).

III. COCHLEAR MICROMECHANICS

The micromechanical domain interfaces to the macromechanical domain through the cochlear partition (BM) boundary condition, Eq. (7). The micromechanical approximation of the BM cross section is typically a lumped mass, stiffness, and damping (per unit area) at each respresented position along the partition. Longitudinal coupling between adjacent cross sections is provided entirely through the fluid and not directly through the BM. This is an important simplification and is justified by the fact that the longitudinal stiffness of BM has been observed to be much smaller than the transverse stiffness in a fresh preparation (Voldřich, 1978). A point-impedance characterization of BM micromechanics can be derived from a representation of BM as an anisotropic plate (Allen and Sondhi, 1979) or a series of progressively broader, viscoelastic beams (Diependaal and Viergever, 1983).

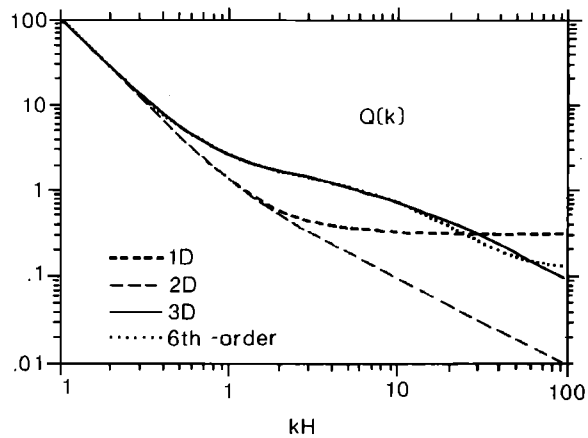

FIG. 3. Relative fluid inertial loading on the cochlear partition as a function of (kH), where k is the wavenumber of spatial distributions in the x dimension and H is the height of each cochlear channel in the y dimension. The function $Q(k)$ is nondimensional and defined in the text as relative fluid inertia. The solid line shows Q_{3D} for the full three-dimensional "box" model. The long-dashed line shows Q_{2D} for a model with two-dimensional fluid mechanics. The short-dashed line shows Q_{1D} for a one-dimensional long-wave approximation to the two-dimensional model. The dotted line shows Q_6 for a sixth-order (in x) curve fit to the solid line Q_{3D}.

The high sensitivity and sharp tuning of single auditory nerve fibers have been regarded by many as an indication that there is more to cochlear micromechanics than just the basilar membrane. Modeling efforts have given consideration to such possibilities as multiple bending modes for the basilar membrane (Steele, 1980), longitudinal stiffness of the tectorial membrane (Zwislocki and Kletsky, 1979), and resonant tectorial-membrane-stereocilia systems (Allen, 1980; Zwislocki and Kletsky, 1980).

If the micromechanics are assumed to have a passive representation (i.e., no local sources of mechanical energy) in a mathematical model of the cochlea, then numerical solutions for basilar membrane displacement in the model provide a reasonable representation of a *postmortem* cochlea (Kim *et al.*, 1980). However, direct measurements of basilar membrane motion (Rhode, 1973; Khanna and Leonard, 1982; Sellick *et al.*, 1982) suggest that *in vivo* micromechanics differ significantly from *postmortem* micromechanics. Recent measurements indicate that basilar membrane displacements are sharply tuned and have frequency responses very similar (but not identical) to those typically measured in single auditory nerve fibers (see Neely and Kim, 1983 for one such comparison).

In order to further investigate hypotheses concerning cochlear function, it is useful to have a model of cochlear mechanics which has BM displacements with the following attributes: (1) sharp tuning similar to that typical of neural measurements, (2) response latency at or below that typical of neural measurements, and (3) peak amplitudes of about 1 nm or greater at the threshold of hearing. It is assumed that these attributes are appropriate for a model of cochear mechanics. Both empirical observations (Neely and Kim, 1983) and mathematical analysis (de Boer, 1983) of cochlear models suggest that it is not possible for a cochlear model to have these attributes unless active elements (mechanical generators) are allowed to exist in the cochlear partition. In other words, a special "cochlear amplifier" is required in order to provide high sensitivity and sharp tuning to BM displacements. [The use of the term "cochlear amplifier" to describe the role of active elements in the cochlea was first suggested by Davis (1983).]

A current view is that the cochlear amplifier is realized by means of a BM displacement to the outer-hair-cell (OHC) membrane potential feedback loop (Weiss, 1982; Mountain *et al.*, 1983). This view requires bidirectional electromechanical transduction within the organ of Corti, probably in the outer hair cells. There is considerable evidence to indicate that hair cells have a "displacement-to-receptor potential" transducer; evidence for a "receptor potential-to-displacement" transducer is accumulating (e.g., Brownell, 1983). We can use a cochlear model to investigate what attributes this hypothetical feedback loop must have to be consistent with experimental observation.

In order for the feedback loop to provide the function of a tuned amplifier, there must be a second frequency-dependent element in addition to the basilar membrane (BM). Analysis of measurements of BM displacements indicates that this second tuned element should add stiffness to BM impedance at each position for low frequencies, contribute "negative damping" over narrow ranges of intermediate frequencies, and have negligible influence at high frequencies. One possible implementation of this type of feedback loop is to indicate an additional term $K_3\xi_2$ in the basilar membrane boundary condition:

$$p_d = M_1\ddot{\xi}_1 + R_1\dot{\xi}_1 + K_1\xi_1 + K_3\xi_2, \tag{16}$$

where $p_d(x,t)$ represents a weighted average of pressure difference across the width of the cochlear partition (see Appendix A); $\xi_1(x,t)$ is the displacement of the partition averaged across the y dimension; and $M_1(x)$, $R_1(x)$, and $K_1(x)$ are the lumped mass, damping, and stiffness of the basilar membrane, respectively. (The dots above the symbols indicate derivatives with respect to time.) The "displacement" of the second tuned system ξ_2 will be a low-pass-filtered version of ξ_1:

$$0 = M_2\ddot{\xi}_2 + R_2\dot{\xi}_2 + K_2\xi_2 - \gamma K_3\xi_1. \tag{17}$$

Equation (15) is written as if the second tuned system were mechanical; this was done mainly for simplicity. It is not yet clear whether OHC tuning should be electrical, mechanical, or both (Weiss, 1982). The necessary transduction to and from electrochemical domain is lumped here in the dimensionless parameter, γ. Figure 4 is a block diagram showing cochlear micromechanics as described by Eqs. (16) and (17).

A more realistic description of cochlear micromechanics would include nonlinear mechanical-to-electrical transduction and electrical-to-mechanical transduction (i.e., Koshigoe and Tubis, 1983). In a nonlinear micromechanical model, amplitude compression (automatic gain control) would be an important function of the cochlear amplifier. We expect that the mechanical energy delivered to the cochlear fluid by this amplifier is also the source of observable cochlear acoustic emissions (Kemp, 1978).

IV. MODEL RESULTS

Numerical results are presented in this section for a mathematical model of cochlear mechanics which includes

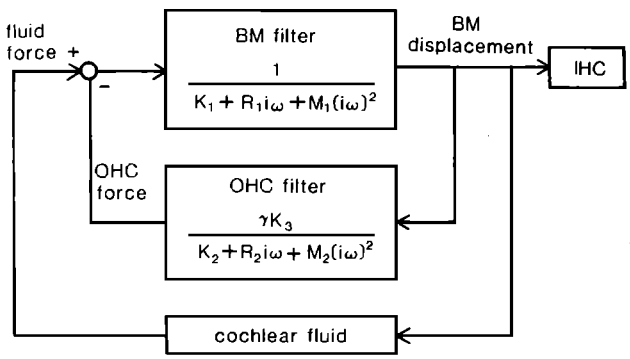

FIG. 4. Feedback model for active elements in the cochlea. The inner hair cells (IHC) are driven by basilar membrane (BM) displacement. The BM filter has a low-pass characteristic and is driven by a combination of fluid force (due to pressure difference across the BM) and outer hair cell (OHC). The OHC filter also has a low-pass characteristic and is driven by BM displacement. Transduction from mechanical-to-electrochemical domain and from electrochemical-to-mechanical domain is thought to be a part of the OHC filter. Longitudinal coupling between adjacent positions on BM is provided by the cochlear fluid.

some of the macromechanical and micromechanical features described in Secs. II and III. The model is a linear, two-dimensional, time-domain representation of the cochlea with active elements in the cochlear partition. The micromechanical equations used here differ from the ones presented in Sec. III in that the feedback loop is implemented using velocity terms instead of displacement terms. Further details concerning the model parameters and form of the basilar membrane point-impedance equation are given by Neely (1983).

The model used to obtain the results shown in this section included a simple representation for earphone, coupler, and middle ear, in addition to the macromechanics and micromechanics of the cochlea. The model parameters for the middle ear and cochlea were chosen to simulate a cat. The stimulus was specified as an impulsive (click) voltage to the earphone.

In Fig. 5, model results for basilar membrane displacement are compared with measurements of discharge patterns in single auditory nerve fibers (Allen, 1983). The solid line curves were obtained by computing discrete Fourier transforms of 20-ms impulse responses for basilar displacement in the model at four positions: 20%, 40%, 60%, and 80% of the length of the basilar membrane from the apex.

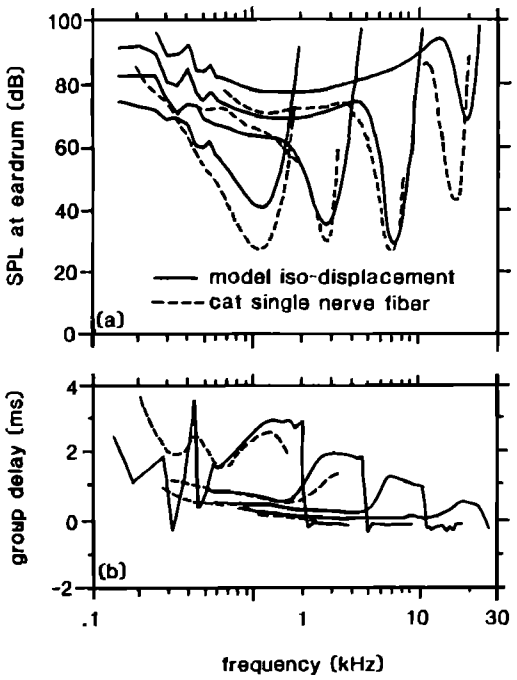

FIG. 5. Comparison between basilar membrane displacement in the model and single nerve fiber discharge in the cat. (a) The solid lines indicate the sound-pressure level required at the eardrum to achieve criterion displacement of 1 nm in ξ_1 (see text) at four places along the length of the cochlea. The dashed lines indicate the sound pressure level required at the eardrum to increase the discharge rate of four single auditory nerve fibers in a cat by 1 spike per 50-ms tone burst as measured by Allen (1983). (b) The solid lines indicate the group delay (defined as the negative of the derivative of the phase with respect to frequency) of basilar membrane displacement in the model relative to eardrum pressure. The dashed lines indicate group delay of neural response relative to stimulus voltage for three of the four nerve fibers shown above with an arbitrary constant of 1.2 ms subtracted. The 1.2-ms adjustment improves the agreement between the model and neural measurements and is attributed to acoustic, synaptic, and neural propagation delays which are not included in the model.

The isodisplacement curve in Fig. 5(a) shows the sound pressure level at the eardrum needed to produce 1 nm (average) displacement of the cochlear partition. The group delay in Fig. 5(b) is defined as minus the derivative with respect to frequency of the phase of the response relative to the stimulus.

The dashed line in Fig. 5(b) represents the sound pressure level needed to increase the discharge rate of four nerve fibers in one cat by 1 spike per 50-ms tone burst. Group delay was computed by Allen (1983) for three of the same nerve fibers for frequencies below about 3.5 kHz. The neural group delay is shown in Fig. 5(b) with 1.2 ms subtracted; this downward shift of the neural group delay curves provided a closer correspondence with model results and can be attributed to acoustic and neural delays not present in the model.

The model results for BM displacement in Fig. 5 are not an exact match to the single nerve fiber tuning curves, but are sufficiently close to say that the model exhibits neural-like tuning. The sharp tuning and high sensitivity shown in the model are a direct result of the cochlear amplifier feedback loop. The "tips" of the model isodisplacement curves would be removed completely if this feedback loop were disabled. The parameters were chosen deliberately to reduce the sensitivity of the model at the low- and high-frequency ends below what was needed to match the neural curves; this was done to avoid problems with unstable model solutions. The model solution shown here was stable in the sense that the transient responses decayed with time. The abrupt changes in value between adjacent data points below 0.6 kHz in Fig. 5 are apparently due to "whole cochlea" resonances which are underdamped in the model.

The characteristic frequency of each of the model curves is in good agreement with the frequency-to-place map determined by Liberman (1982), as shown in Fig. 6. One deficiency of the model is that it did not reproduce the bending seen in Liberman's curve for frequencies below 2 kHz; additional model parameters may be required in order to produce this feature.

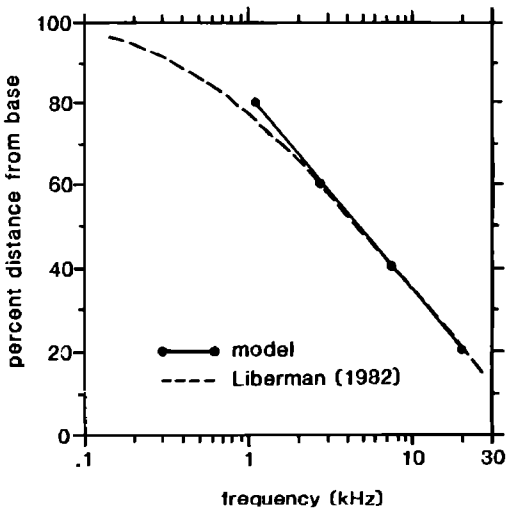

FIG. 6. Cochlear frequency-to-place map. The solid line indicates the relationship between place on the basilar membrane and most sensitive frequency (characteristic frequency) in the model at the four places used for Fig. 5. The dashed line indicates the corresponding frequency-to-place map for cochlear neurons in cat as determined by Liberman (1982).

The model results are encouraging, but the model still needs much refinement: (1) some of the macromechanical and micromechanical features mentioned in Secs. II and III have not yet been incorporated into the model, (2) the inclusion of a nonlinear parameter (probably γ) to provide amplitude compression will be an important step, (3) the model representation of bidirectional transduction tuning should be more explicit, and (4) numerical methods need to be refined to minimize computation time.

Realistic computer simulations of cochlear mechanics are possible and important to hearing research. Mathematical modeling of cochlear mechanics can provide new insights to improve our understanding of developing and impaired cochlear function as well as helping us to identify the essential features of normal cochlear function.

V. SUMMARY

Analytical techniques have been developed in the past few years to overcome the long- or short-wave limitations of earlier cochlear models. It is now possible to model the cochlear fluid over the entire range of wavelengths important to cochlear mechanics. Solution methods can be analyzed and evaluated in terms of their relative fluid inertial loading on the partition as a function of wavenumber.

It seems increasingly plausible that a cochlear amplifier provides the high sensitivity and sharp tuning normally associated with the cochlea. This cochlear amplifier may be implemented by a feedback loop, which includes transduction from electrical potential-to-mechanical force as well as transduction from mechanical displacement-to-electrical potential. Both transduction elements are thought to be located in the vicinity of the outer hair cells.

Active models of cochlear mechanics can simulate neural-like tuning in basilar membrane displacements. Passive models can simulate basilar membrane displacements typical of *postmortem* measurements. Mathematical models of cochlear mechanics are developing rapidly as computational resources become available to provide numerical solutions.

ACKNOWLEDGMENTS

Many of the ideas included in this paper were previously presented by participants of the IUTAM/ICA symposium on Mechanics of Hearing in July 1983 at Delft University of Technology, Delft, The Netherlands. Arnold Tubis (Purdue University) provided suggestions which helped to improve the mathematical presentation in this paper.

APPENDIX A: DERIVATION OF $Q(k)$

The function $Q(k)$ describes a realtionship between the spatial Fourier components of $\xi_1(x)$ and $p_d(x)$. We will define p_d as a weighted average of pressure differences p over the width of the partition.

$$p_d(x) = \frac{1}{\zeta_0 W}\int_{-W/2}^{W/2} p(x,y,0)\zeta(y)dy. \tag{A1}$$

The definition of p_d should properly scale energy flow between macromechanics and micromechanics. When the stapes boundary is moving with acceleration $\ddot{\xi}_s$, $\eta(y,z)$, then $p(x,y,z)$ can be represented by a series expression of the form

$$\begin{aligned} p(x,y,x) = &\sum_{m=-\infty}^{\infty}\sum_{n=-\infty}^{\infty} P_{mn}\cos\left(\frac{n\pi}{L}x\right) \\ &\times\cos\left(\frac{m\pi}{W}y\right)\cosh\beta_{mn}(H-z) \\ &+\sum_{m=-\infty}^{\infty}\sum_{n=-\infty}^{\infty}\tilde{P}_{mn}\sin\left(\frac{(n+1/2)\pi}{L}x\right) \\ &\times\cos\left(\frac{m\pi}{W}y\right)\cosh\tilde{\beta}_{mn}(H-z), \end{aligned} \tag{A2}$$

where

$$\beta_{mn} = [(n\pi/L)^2 + (m\pi/W)^2]^{1/2}, \tag{A3}$$

$$\tilde{\beta}_{mn} = \{[(n+1/2)\pi/L]^2 + (m\pi/W)^2\}^{1/2}. \tag{A4}$$

The reader should note that the series expression in Eq. (A2) satisfies Laplace's equation, the apical boundary condition, and the upper wall boundary condition, and places some constraints on the form of $\eta(y,z)$. Substituting Eq. (A2) into Eq. (A1) gives

$$\begin{aligned} p_d(x) = &\sum_{m=-\infty}^{\infty}\left[\sum_{n=-\infty}^{\infty} P_{mn}\left(\frac{\zeta_m}{\zeta_0}\right)\cosh\beta_{mn}H\right]\cos\left(\frac{n\pi}{L}x\right) \\ &+\left[\sum_{n=-\infty}^{\infty}\tilde{P}_{mn}\left(\frac{\zeta_m}{\zeta_0}\right)\cosh\tilde{\beta}_{mn}H\right] \\ &\times\sin\left(\frac{(n+1/2)\pi}{L}x\right). \end{aligned} \tag{A5}$$

We assume that $\ddot{\xi}_1$ and ζ can be represented by similar series representations

$$\ddot{\xi}_1(x) = \frac{1}{\zeta_0}\sum_{n=-\infty}^{\infty}\alpha_n\cos\left(\frac{n\pi}{L}x\right) + \tilde{\alpha}_n\sin\left(\frac{(n+1/2)\pi}{L}x\right), \tag{A6}$$

$$\zeta(y) = \sum_{m=-\infty}^{\infty}\zeta_m\cos\left(\frac{m\pi}{W}y\right). \tag{A7}$$

From the partition boundary, Eq. (7), we have a relationship between $\ddot{\xi}_1$ and p

$$\begin{aligned} \ddot{\xi}_1(x)\zeta(y) = \frac{1}{2\rho}\frac{\partial}{\partial z}p(x,y,0) = &-\frac{1}{2\rho} \\ &\times\sum_{m=-\infty}^{\infty}\left[\sum_{n=-\infty}^{\infty} P_{mn}\beta_{mn}\sinh\beta_{mn}H\cos\left(\frac{n\pi}{L}x\right)\right. \\ &\left.+\tilde{P}_{mn}\tilde{\beta}_{mn}\sinh\tilde{\beta}_{mn}H\sin\left(\frac{(n+1/2)\pi}{L}x\right)\right] \\ &\times\cos[(m\pi/W)y]. \end{aligned} \tag{A8}$$

Using Eqs. (A6)–(A8) we can solve for P_{mn} and $\tilde{P}_{mn}$ in terms of α_n and $\tilde{\alpha}_n$

$$P_{mn} = (\zeta_m/\zeta_0)(2\rho\alpha_n/\beta_{mn}\sinh\beta_{mn}H), \tag{A9}$$

$$\tilde{P}_{mn} = (\zeta_m/\zeta_0)(2\rho\tilde{\alpha}_n/\tilde{\beta}_{mn}\sinh\tilde{\beta}_{mn}H). \tag{A10}$$

Substituting Eqs. (A9) and (A10) into Eq. (A5) gives

$$\begin{aligned} p_d(x) = &-2\rho H\sum_{n=-\infty}^{\infty}\alpha_n Q\left(\frac{n\pi}{L}\right)\cos\left(\frac{n\pi}{L}x\right) \\ &+\tilde{\alpha}_n Q\left(\frac{(n+1/2)\pi}{L}\right)\sin\left(\frac{(n+1/2)\pi}{L}x\right), \end{aligned} \tag{A11}$$

where we define the function Q as

$$Q\left(\frac{n\pi}{L}\right)=\sum_{n=-\infty}^{\infty}\left(\frac{\zeta_m}{\zeta_0}\right)^2\frac{\coth\beta_{mn}H}{\beta_{mn}H}. \tag{A12}$$

The hyperbolic cotangent also has a series representation (Gradshteyn and Ryzhik, 1965):

$$\frac{\coth\beta_{mn}H}{\beta_{mn}H}=\sum_{l=-\infty}^{\infty}\frac{1}{(\beta_{mn}H)^2+(l\pi)^2}$$
$$=\sum_{l=-\infty}^{\infty}\left[\left(\frac{n\pi}{L}H\right)^2+\left(\frac{m\pi}{W}H\right)^2+(l\pi)^2\right]^{-1}. \tag{A13}$$

Finally, we substitute Eq. (A13) into Eq. (A12) and let $k=(n\pi/L)$ to obtain Eq. (10) for $Q_{3D}(k)$.

APPENDIX B: DIFFERENTIAL EQUATION FOR THE 1-D LONG-WAVE APPROXIMATION

Using the one-dimensional (1D) long-wave approximation for $Q(k)$ from Eq. (14) and the series expression for p_d from Eq. (A11) we can derive a differential equation relating p_d and ξ_1 which is second order in x:

$$\frac{d^2}{dx^2}p_d(x)=\frac{2\rho\zeta_0}{H}\ddot{\xi}_1(x)-\frac{2}{3}\rho H\zeta_0\frac{d^2}{dx^2}\ddot{\xi}_1(x). \tag{B1}$$

In a frequency-domain formulation we can relate $\dot{\xi}_1(x)$ to $p_d(x)$ by defining the cochlear partition impedance $Z(x)$. From Eqs. (A6) and (A11) and assumed $e^{i\omega t}$ harmonic time dependence

$$Z(x)=\frac{p_d(x)}{\dot{\xi}_1(x)}=\left[-2\rho H\sum_{n=-\infty}^{\infty}\alpha_n Q\left(\frac{n\pi}{L}\right)\cos\left(\frac{n\pi}{L}x\right)\right.$$
$$\left.+\tilde{\alpha}_n Q\left(\frac{(n+1/2)\pi}{L}\right)\sin\left(\frac{(n+1/2)\pi}{L}x\right)\right]$$
$$\times\left[\frac{1}{i\omega\zeta_0}\sum_{n=-\infty}^{\infty}\alpha_n\cos\left(\frac{n\pi}{L}x\right)\right.$$
$$\left.+\tilde{\alpha}_n\sin\left(\frac{(n+1/2)\pi}{L}x\right)\right]^{-1}. \tag{B2}$$

This is a discretized version of the integral equation derived by Siebert (1974), de Boer (1981), and others. With this definition of cochlear partition impedance, we can express Eq. (B1) in the frequency domain as

$$\frac{d^2}{dx^2}\left(p_d(x)\frac{Z(x)+i\omega M_f}{Z(x)}\right)=\frac{2i\omega\rho\zeta_0}{H}\frac{p_d(x)}{Z(x)}, \tag{B3}$$

where

$$M_f=(2/3)\rho H\zeta_0 \tag{B4}$$

is the fluid mass (per unit area) which rides with the partition. Equation (B3) is the well-known differential equation for the 1-D long-wave approximation. For an alternative derivation of this differential equation (starting from an integral equation) see Sondhi (1978).

If the micromechanics are described by Eqs. (16) and (17), then the cochlear partition impedance is

$$Z(x)=i\omega M_1+R_1+(K_1/i\omega)$$
$$+\gamma(K_3/i\omega)^2/(i\omega M_2+R_2+K_2/i\omega). \tag{B5}$$

The mechanical parameters for mass, stiffness, and damping in Eq. (B5) must be chosen in order to solve for p_d in Eq. (B3). The form of $Z(x)$ may be different for other models of cochlear micromechanics.

Allen, J. B. (1977). "Cochlear micromechanics—a method for transforming mechanical to neural tuning within the cochlea," J. Acoust. Soc. Am. **62**, 930–939.

Allen, J. B. (1980). "A cochlear micromechanical model of transduction," in *Psychological, Physiological and Behavioural Studies in Hearing*, edited by G. van den Brink and F. A. Bilsen (Delft U.P., Delft, The Netherlands), pp. 85–95.

Allen, J. B. (1983). "Magnitude and phase-frequency response to single tones in the auditory nerve," J. Acoust. Soc. Am. **73**, 2071–2092.

Allen, J. B., and Sondhi, M. M. (1979). "Cochlear macromechanics: Time-domain solutions," J. Acoust. Soc. Am. **66**, 123–132.

Boer, E. de (1980). "Auditory physics. Physical principles in hearing I," Phys. Rep. **62** (2), 87–274.

Boer, E. de (1981). "Short waves in three-dimensional cochlear models: Solution for a 'block' model," Hear. Res. **4**, 53–77.

Boer, E. de (1983). "No sharpening? A challenge for cochlear mechanics," J. Acoust. Soc. Am. **73**, 567–573.

Boer, E. de (1984). "Auditory physics. Physical principles in hearing II," Phys. Rep. **105** (3), 141–226.

Boer, E. de, and van Bienema, E. (1982). "Solving cochlear mechanics problems with higher order differential equations," J. Acoust. Soc. Am. **72**, 1427–1434.

Brownell, W. E. (1983). "Observation on a motile response in isolated outer hair cells," in *Mechanisms on Hearing*, edited by W. R. Webster and L. M. Aitkin (Monash U.P., Clayton, Victoria, Australia), pp. 5–10.

Davis, H. (1983). "An active process in cochlear mechanics," Hear. Res. **9**, 79–90.

Diependaal, R. J., and Viergever, M. A. (1983). "Point impedance characterization of the basilar membrane in a three-dimensional cochlear model," Hear. Res. **11**, 33–40.

Gradshteyn, I. S., and Ryzhik, I. M. (1965). *Table of Integrals, Series, and Products* (Academic, New York), p. 36, Eq. 1.421.4.

Hall, J. L. (1974). "Two-tone distortion products in a nonlinear model of the basilar membrane," J. Acoust. Soc. Am. **56**, 1818–1828.

Kemp, D. T. (1978). "Stimulated acoustic emissions from within the human auditory system," J. Acoust. Soc. Am. **64**, 1386–1391.

Khanna, S. M., and Leonard, D. G. B. (1982). "Basilar membrane tuning in the cat cochlea," Science **215**, 305–306.

Kim, D. O., Molnar, C. E., and Pfeiffer, R. R. (1973). "A system of nonlinear differential equations modeling basilar membrane motion," J. Acoust. Soc. Am. **54**, 1517–1529.

Kim, D. O., Neely, S. T., Molnar, C. E., and Matthews, J. W. (1980). "An active cochlear model with negative damping in the partition: Comparison with Rhode's ante- and post-mortem observation," in *Psychological, Physiological and Behavioural Studies in Hearing*, edited by G. van den Brink and F. A. Bilsen (Delft U.P., Delft, The Netherlands), pp. 7–14.

Koshigoe, S., and Tubis, A. (1983). "A non-linear feedback model for outer hair cell stereocilia and its implication for the response of the auditory periphery," in *Mechanics of Hearing*, edited by E. de Boer and M. A. Viergever (Delft U.P., Delft, The Netherlands), pp. 127–134.

Lesser, M. B., and Berkley, D. A. (1972). "Fluid mechanics in the cochlea: Part 1," J. Fluid Mech. **51**, 497–512.

Liberman, M. C. (1982). "The cochlear frequency map for the cat: Labeling auditory-nerve fibers of known characteristic frequency," J. Acoust. Soc. Am. **72**, 1441–1449.

Lighthill, J. (1981). "Energy flow in the cochlea," J. Fluid Mech. **106**, 149–213.

Loh, C. H. (1983). "Multiple scale analysis of the spirally coiled cochlea," J. Acoust. Soc. Am. **74**, 95–103.

Matthews, J. W. (1980). "Mechanical modeling of nonlinear phenomenon observed in the peripheral auditory system," Doctoral dissertation (Washington University, St. Louis, MO).

Matthews, J. W. (1983). "Modeling reverse middle ear transmission of acoustic distortion signals," in *Mechanics of Hearing*, edited by E. de Boer and M. A. Viergever (Delft U.P., Delft, The Netherlands), pp. 11–18.

Mountain, D. C., Hubbard, A. E., and McMullen, T. A. (**1983**). "Electrochemical processes in the cochlea," in *Mechanics of Hearing*, edited by E. de Boer and M. A. Viergever (Delft U.P., Delft, The Netherlands), pp. 119–126.

Neely, S. (**1981**). "Finite difference solution of a two-dimensional mathematical model of the cochlea," J. Acoust. Soc. Am. **69**, 1386–1392.

Neely, S. (**1983**). "The cochlear amplifier," in *Mechanics of Hearing*, edited by E. de Boer and M. A. Viergever (Delft U.P., Delft, The Netherlands), pp. 111–118.

Neely, S. T., and Kim, D. O. (**1983**). "An active cochlear model showing sharp tuning and high sensitivity," Hear. Res. **9**, 123–130.

Petersen, L. C., and Bogert, B. P. (**1950**). "A dynamical theory of the cochlea," J. Acoust. Soc. Am. **22**, 369–381.

Rhode, W. S. (**1973**). "An investigation of post-mortem cochlear mechanics using the Mössbauer effect," in *Basic Mechanisms in Hearing*, edited by A. R. Moller (Academic, New York), pp. 49–67.

Rhode, W. S. (**1978**). "Some observations on cochlear mechanics," J. Acoust. Soc. Am. **64**, 158–176.

Sellick, P. M., Patuzzi, R., and Johnstone, B. M. (**1982**). "Measurement of basilar membrane motion in the guinea pig using the Mössbauer technique," J. Acoust. Soc. Am. **72**, 131–141.

Siebert, W. A. (**1974**). "Ranke revisited—a simple short-wave cochlear model," J. Acoust. Soc. Am. **56**, 594–600.

Sondhi, M. H. (**1978**). "Method for computing motion in a two-dimensional cochlear model," J. Acoust. Soc. Am. **61**, 110–119.

Steele, C. R. (**1980**). "Lecture notes on cochlear mechanics," NSF-CBMS Regional Conference on Mathematical Models of the Hearing Process, Rensselaer Polytechnic Institute, Troy, NY (unpublished).

Steele, R. C., and Tabor, L. A. (**1979**). "Comparison of WKB calculations and experimental results for 3-D cochlear models," J. Acoust. Soc. Am. **65**, 1007–1111.

Viergever, M. A. (**1980**). *Mechanics of the Inner Ear—a Mathematical Approach* (Delft U. P., Delft, The Netherlands).

Voldřich, L. (**1978**). "Mechanical properties of basilar membrane," Acta Otolaryngol. **86**, 331–335.

Weiss, T. F. (**1982**). "Bidirectional transduction in vertebrate hair cells: A mechanism for coupling mechanical and electrical processes," Hear. Res. **7**, 353–360.

Zwislocki, J. J. (**1950**). "Theory of acoustical action in the cochlea," J. Acoust. Soc. Am. **22**, 778–784.

Zwislocki, J. J., and Kletsky, E. J. (**1979**). "Tectorial membrane: A positive effect on frequency analysis in the cochlea," Science **204**, 639–641.

Zwislocki, J. J., and Kletsky, E. J. (**1980**). "Micromechanics in the theory of cochlear mechanics," Hear. Res. **2**, 505–512.